Proceedings of the ASME 2020 International Design Engineering Technical Conferences and Computers and Information in Engineering Conference IDETC/CIE2020 August 16-19, 2020, St. Louis, MO, USA

### **DETC2020-22604**

# ORGANIC PIEZORESISTIVE PRESSURE SENSITIVE ROBOTIC SKIN FOR PHYSICAL HUMAN-ROBOT INTERACTION

Danming Wei<sup>1</sup>, Ruoshi Zhang, Mohammad N. Saadatzi, Olalekan O. Olowo, Dan O. Popa Next Generation Systems Lab, Department of Electrical and Computer Engineering, University of Louisville, Kentucky, USA

#### **ABSTRACT**

Pressure sensitive robotic skins have long been investigated for applications to physical human-robot interaction (pHRI). Numerous challenges related to fabrication, sensitivity, density, and reliability remain to be addressed under various environmental and use conditions. In our previous studies, we designed novel strain gauge sensor structures for robotic skin arrays. We coated these star-shaped designs with an organic polymer piezoresistive material, Polv ethylenedioxythiophene)-ploy(styrenesulfonate) or PEDOT: PSS and integrated sensor arrays into elastomer robotic skins. In this paper, we describe a dry etching photolithographic method to create a stable uniform sensor layer of PEDOT:PSS onto starshaped sensors and a lamination process for creating doublesided robotic skins that can be used with temperature compensation. An integrated circuit and load testing apparatus was designed for testing the resulting robotic skin pressure performance. Experiments were conducted to measure the loading performance of the resulting sensor prototypes and results indicate that over 80% sensor yields are possible with this fabrication process.

Keywords: pHRI, robotic skin sensor, PEDOT:PSS, fabrication, lamination

#### 1. INTRODUCTION

For decades, artificial robotic skin has attracted the interest among researchers, especially for applications in physical human-robot interaction and autonomous manipulation[1, 2]. The sense of touch enables robots to physically interact with their environment and people, in applications such as grasping manipulation[3] and full-body haptic sensing[4]. Many

In the past several years, we have been investigating and developing robotic skin sensor arrays based on semiconductor organic materials, and addressing challenges in design, simulation[11], fabrication[12], packaging[13], electronic transducers, interfaces to robot controllers, and human-robot interaction algorithms[14]. The base sensing material used in our research is the organic semiconductor polymer Poly (3, 4-ethylenedioxythiophene)-ploy(styrenesulfonate) or PEDOT: PSS, that has been printed over flexible Kapton substrate using several techniques. The active sensor material changes resistance in response to strain and it is consistent with a 20:1 gauge factor[11].

In [15], we used Electro-Hydro-Dynamic (EHD) ink jetting to print mm-size interdigitated strain gauge structures with 10 micron feature resolution. Under a high voltage electrical field working environment, the EHD print head has to be a specialized nozzle. However, the inks for EHD printing must have special formulations to satisfy conductivity and viscosity requirements, and the printing process is highly serial in nature, e.g. one gauge is printed at a time. In[15], the sensor geometry included interdigitated designs, resulting in directional pressure sensitivity in the vicinity of the sensor.

In [12], we investigated a scalable, cleanroom compatible fabrication technique using spinning and wet lift-off

© 2020 by ASME

researchers have investigated robotic skins design that match or outperform humans, incorporating temperature and pressure sensors using different transducer mechanisms including: capacitive sensing[5], conductive fabrics[6], infrared sensors[7], or semiconductor strain gauges[8]. However, after over 30 years of research, numerous challenges related to fabrication and integration of skin sensors with robots remain[9, 10].

<sup>&</sup>lt;sup>1</sup> Danming Wei: danming.wei@louisville.edu

photolithography. In addition, the sensor geometry employed was a star-shaped strain gauge structure incorporated in a 4x4 skin sensor array. In[12], the star-shaped sensor structure had a circular symmetric pressure response and was thoroughly characterized by indentation experiments.

The wet lift-off photolithographic method improved the deposition process when compared to EHD printing but required Acetone to lift-off unnecessary sensing film. In addition, the process required spinning PEDOT:PSS solution diluted with Methanol with ratios between 1:1 and 1:4[12]. During the process, PEDOT:PSS residue cannot be removed perfectly but remains on the sensing areas, therefore affecting the conductivity and sensitivity of the sensors. In particular, if arrays of tactile sensors are produced, they will have wide variations in resistance, which require additional lamination and calibration procedures. An example of a resulting sensor sample is shown in Figure 1, where 5 of 16 tactile sensors will not perform properly due to lift-off process imperfections.

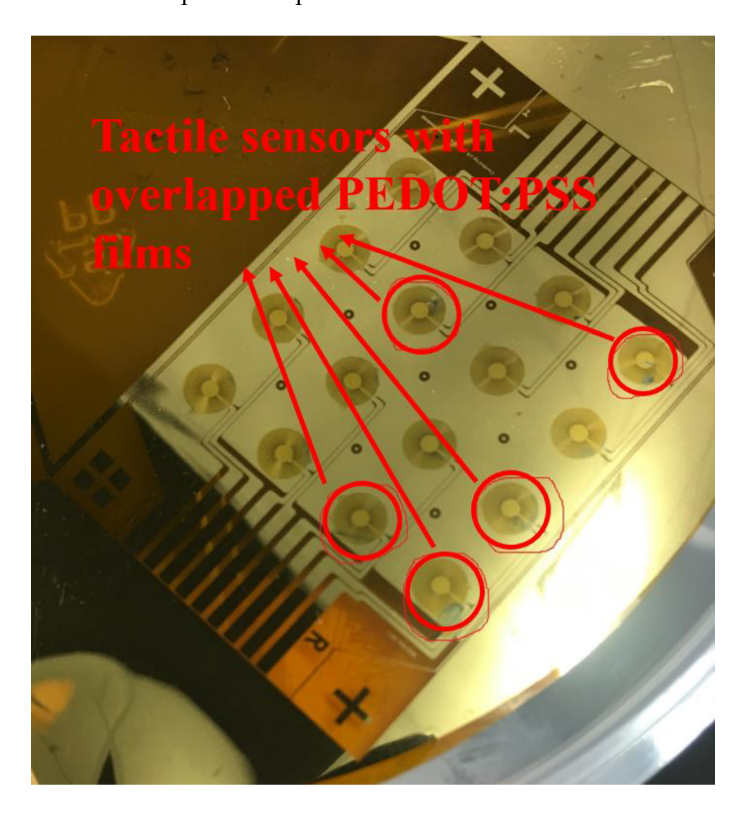


**FIGURE 1:** OVERLAPPED PEDOT:PSS MATERIAL ON A 4X4 SKIN SENSOR ARRAY, RESULTING IN 5 TACTILE SENSORS WITH POOR PERFORMANCE

To solve this problem, in this paper, we propose a new dry etching photolithographic process which can repeatably deposit uniform PEDOT:PSS sensing layers. The process does not require Methanol additives. Instead, a new formulation of PEDOT:PSS with Dimethyl sulfoxide (DMSO) and Polyvinylpyrrolidone (PVP) was investigated. The presence of the new additives increases the tactile sensors resistance and results in better sensitivity. In addition, to protect the sensing

area, a physical cap was created to deposit a protective Titanium layer. As a result, the lift-off process which contributed to residue on the sensing elements was replaced with dry etching and results in more repeatable sensor characteristics.

This paper is organized as follows: Section 2 describes skin sensor array design, fabrication and lamination process, as well as the formulation of a new PEDOT:PSS mixture solution; in Section 3, we present the experimental measurement system to carry out electrical and mechanical measurements of the resulting sensor array; in Section 4, the experimental results are presented and discussed to evaluate the corresponding stain gauge performance after applying the different loads on sensing areas; in Section 5, we conclude the paper and discuss future work.

## 2. FABRICATION AND LAMINATION PROCESS 2.1 Sensor design

The star-shaped tactile sensors in our design have been simulated using COMSOL® Finite Element Analysis (FEA), as described in [16]. Here, we summarized the dimensional parameters of our sensor array used to refine the fabrication process. A photolithographic mask was generated as depicted in Figure 2. The mask has three sensor arrays and each array has 16 individual tactile sensor in 4x4 arrangement. The diameter of each sensor is 3.65mm and the 16 sensors are arrayed in a grid with each sensor separated by 7mm spacing. Figure 2 also depicts the dimensions of a single beam in star-shaped structure. Electrical traces are 0.5mm apart and they are 1mm thick. Nine electrodes are interconnected from tactile sensors to both sides of the array. Eight electrodes are for signal lines and one is for ground. The side electrodes will later be used for interconnection to the electronic circuit.

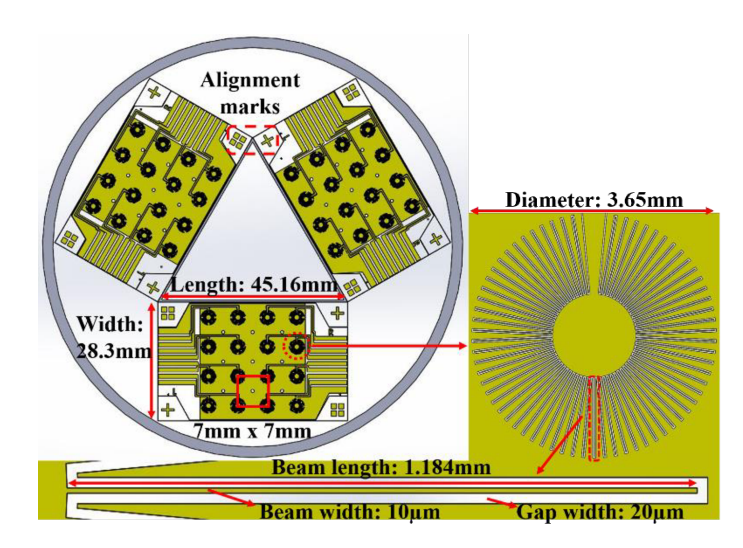


**FIGURE 2:** STAR-SHAPED SENSOR ARRAY MASK DESIGN FOR 4 INCH WAFER AND DIMENSIONS OF SENSOR ARRAY, SINGLE SENSOR AND SINGLE BEAM

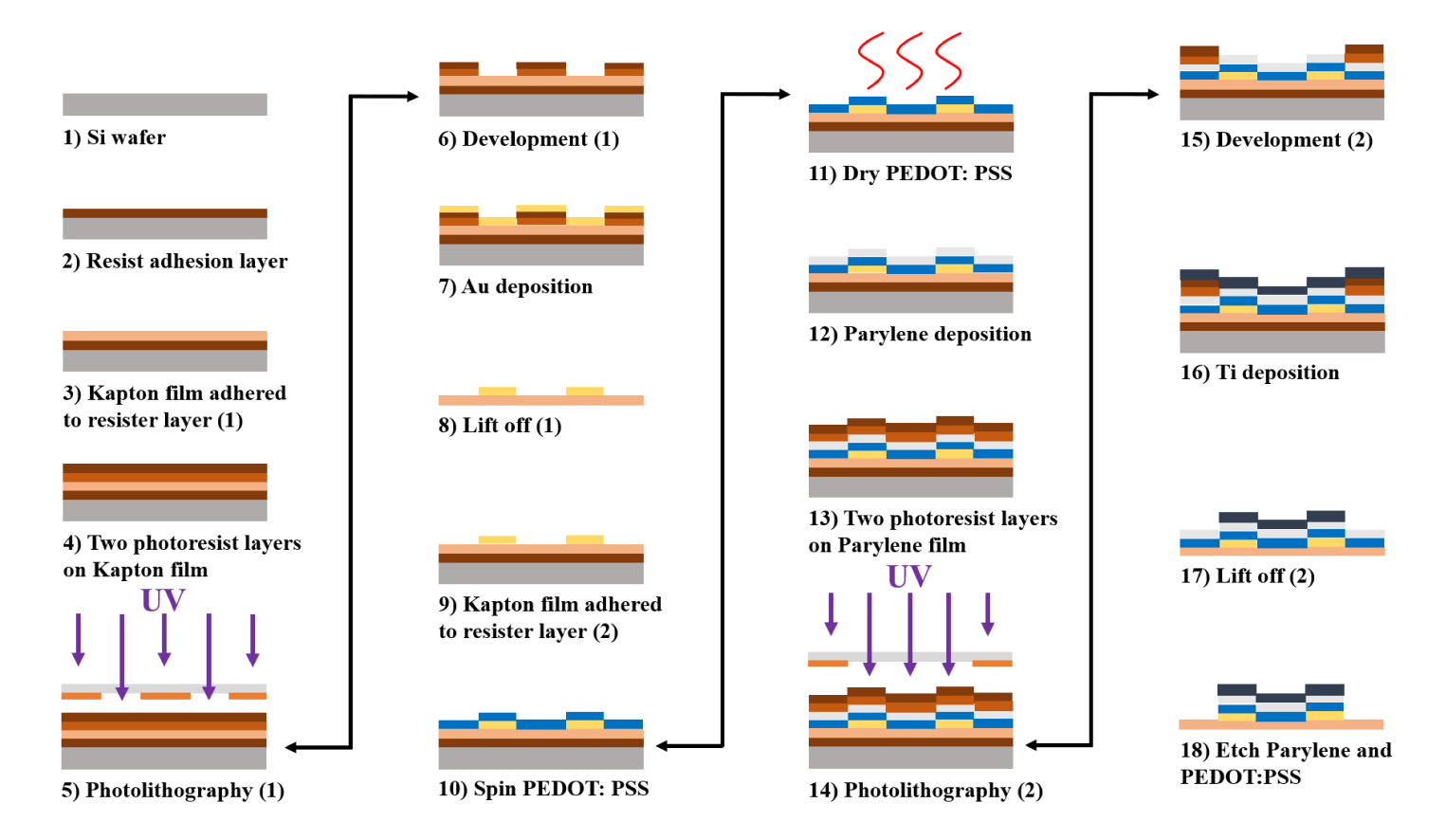


FIGURE 3: SENSOR FABRICATION STEPS, INCLUDING ELECTRODE, PEDOT:PSS DEPOSITION, AND PATTERNING USING DRY-LIFTOFF TECHNIQUE

#### 2.2 Fabrication process

We adapt well-known cleanroom techniques to fabricate the pressure sensitive robotic skin sensor with PEDOT:PSS organic piezoresistive material on Kapton® substrates. Figure 3 depicts the fabrication process leading to patterning of sensor features on 50  $\mu m$  thick Kapton® sheets. To improve the repeatability of PEDOT:PSS deposition and the performance of sensor arrays sensitivity, we developed a dry etching photolithographic method to create a uniform PEDOT:PSS layer on the star-shaped sensing structures.

To make a PEDOT:PSS based solution with high viscosity and more stability, we used two chemical additives: Dimethyl sulfoxide (DMSO) and Polyvinylpyrrolidone (PVP). They are mixed with 5wt% PEDOT:PSS in a ratio of 2g (PEDOT): 2g (DMSO): 0.77g (PVP), which is the quantity needed to fabricate one substrate. Before spinning the PEDOT:PSS mixture solution on the substrate, it should be sonicated for at least 60 seconds in order to evenly generate a uniform sensor layer.

The overall fabrication process is described in detail below: Step 1: First, a clean 4" silicon wafer is prepared as a carrier and spun with MicroChem® SPR 220-3.0 photoresist.

Step 2: A Kapton® polyimide film is cut to an appropriate size, which is a little smaller than the 4" wafer size and cleaned by Acetone and Isopropyl alcohol (IPA), in that order. The film is aligned and loaded on a carrier 4-inch silicon wafer and place

on a hotplate at 115°C for 60 seconds, where the Kapton® film is covered with a 6" by 6" square thicker Kapton® film and laminated by a brayer. The wafer along with the Kapton film is removed after heating for a short time. Take away the thicker Kapton® film and then the skin sensor Kapton® substrate is adhered on the wafer.

Step 3: Two-layer photoresists composed of MicroChem LOR3A and SPR220-3.0 are spun onto the wafer respectively for patterning the electrodes. The wafer is soft baked at 115°C for 120 seconds and cooled down before the next step.

Step 4: Select a desired electrode mask to do first photolithography using a Karl SUSS® mask aligner with 16 seconds UV light exposure.

Step 5: The wafer is then placed on the hotplate at  $115^{\circ}$ C for 60 seconds as post-bake. The photoresist is developed using MF319 developer. Then the sample is dried with  $N_2$  gun and cleaned using MARCH® Reactive Ion Etching (RIE) set at 50 watts power with a 20 SCCM flow rate of Oxygen for 45 seconds under 300 mTorr pressure.

Step 6: A sputtering deposition system, Kurt J. Lesker® PVD75, is used to sputter 300 nm of Gold on the patterned Kapton film. The coated Kapton® film and wafer are placed in a beaker with Acetone, then placed in a sonicated bath for approximately 20 minutes for liftoff. The Kapton® film detaches from the wafer and is rinsed several times with Acetone and IPA and dried with a  $N_2$  gun.

Step 7: Each sensor's resistance is measured before continuing the fabrication process. Ideally, the measured conductance values of each sensor should be zero because they are open circuits. If any sensor has a non-zero conductance value, the Kapton® film will be liftoff again or cleaned by RIE. The reworked film with interdigitated structures should be adhered to a new carrier wafer following step 2.

Step 8: A PEDOT:PSS based solution is spun onto the Kapton® film, and the patterning windows over the interdigitated structures are covered with a semi-conductive material. Then the wafer is moved into a conventional oven to dry at 80°C under vacuum for 10 minutes.

Step 9: The wafer is cooled, then a SCS Labcoter® 2 (PDS 2010) Parylene deposition system is used to coat a thin layer on the Kapton® film with 2g type C Parylene particle. When coating is done, the sensor surface is sprayed with  $N_2$  to remove any dust.

Step 10: Repeat step 3 to spin two layers of MicroChem LOR3A and SPR220-3.0 photoresists on the Parylene film.

Step 11: Using a second mask, the sensor area is exposed to do a second photolithography step in the mask aligner with 16 seconds under UV light, and then repeat step 5.

Step 12: Using the PVD75, a 300nm thickness Titanium is sputtered on the top surface of each tactile sensor. Then repeat the liftoff process in step 6.

Step 13: Finally, the RIE machine is set at 200 watts power with a 20 SCCM flow rate of Oxygen to etch the surface of Kapton® film for several cycles (each cycle is 5 minutes etching and 1-minute cooling) until reach the Kapton® substrate.

Because the etching rate of Titanium is considerably slower than that of Parylene and PEDOT:PSS mixture, the Titanium looks like a cap which can protect PEDOT:PSS remaining in the sensing areas, as shown in Figure 4. At this point, each sensor should have non-zero resistance values and these values are recorded for the pairing process prior to lamination, as described in the next section.

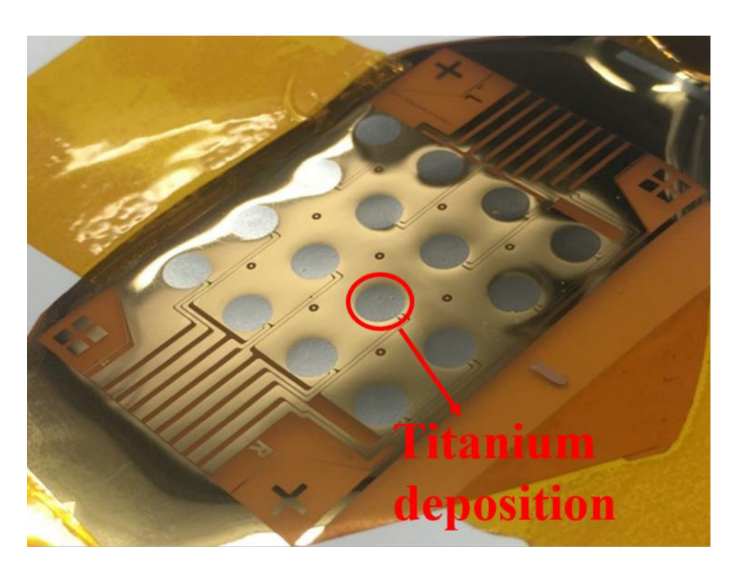


FIGURE 4: THE FABRICATED SKIN SENSOR ARRAY

#### 2.3 Lamination process

After the skin sensor array fabrication is completed, the arrays are prepared for lamination as a double-sided skin structure prior to testing. The purpose of double-sided sensors is to compensate for temperature drifts and also double the sensitivity of the skin, as discussed in detail in our prior work[11].

The overall lamination process is described below:

Step 1: The Kapton® substrate, which was fabricated with star-shaped sensor array structures, is cut in three pieces, as shown in Figure 2. Then, the sensor films are placed in a suitable uncovered container and move them to a conventional oven at 85°C under vacuum for 15 minutes.

Step 2: The samples are handled with care and placed on a flat surface with adhesive tape. Then the samples are evenly protected with a wider Kapton® tape. Both tapes are cut to size while the electrode areas are protected.

Step 3: Based on the measured resistance of tactile sensors, two sensor arrays, whose resistances' values are most closely matched, are selected to form a lamination pair. Then, pick up one of a pair of sensors whose back faces up and place it on the flat substrate. An additional thin Kapton® tape is used to create double layers on both sides of the electrode connectors. Finally, we use a razor blade to remove the extra tape out of the sensor array outline. Because the connection space of a zero-insertion-force (ZIF) connector is wider than two sensor array substrates laminated together, the double layers of thin Kapton® tape are employed to increase the electrodes thickness of double-side sensor array to match the ZIF connector space.

Step 4: Two sensor array of a pair were cleaned with Acetone and IPA, then aligned back to back following the alignment marks placed at the corners of the sensor array. We used a clip to clamp one side of the pair.

Step 5: The double-layer sensor array is placed on the flat substrate, put wiping paper in the middle of the pair and separated them. Then we sprayed 3M® contact adhesive evenly in between the pairs.

Step 6: The wiping paper was removed, and the pair was closed together, then the clip was removed, another wiping paper was placed on the top of the laminated sensor arrays and the brayer was used to create a double-sided structure.

Step 7: Laminated double-layer sensor array is put between two flat substrates, placed a heavy metal block on the top and moved them into the conventional oven at 75°C under vacuum for 10 minutes to cure the adhesive.

Step 8: Finally, the laminated sensor array is moved out and trimmed the outline to make its edge flush with the bottom for inserting two ZIF connectors, which are now ready to interconnect with our conditioning electronic circuit.

Figure 5 depicts the lamination process, including pictures of the 8 steps outlined in this section.

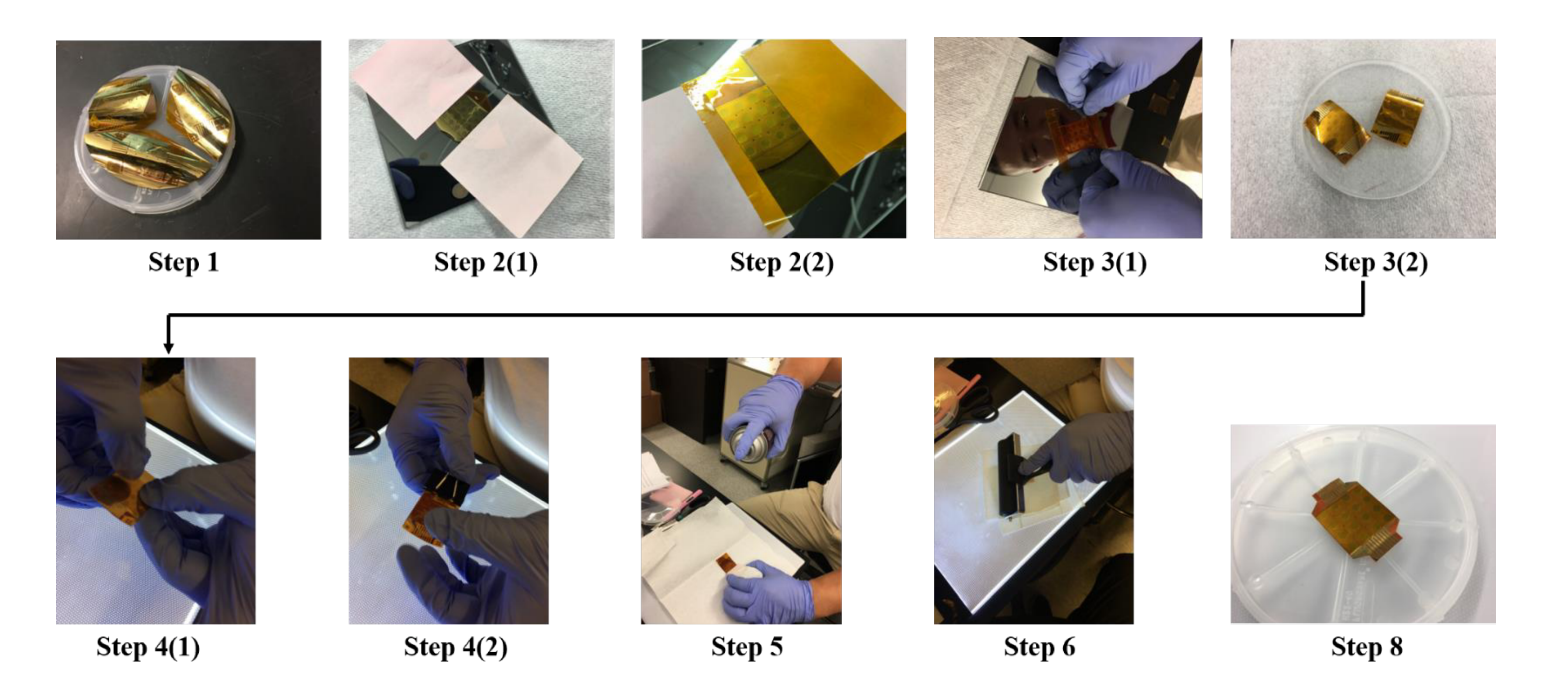
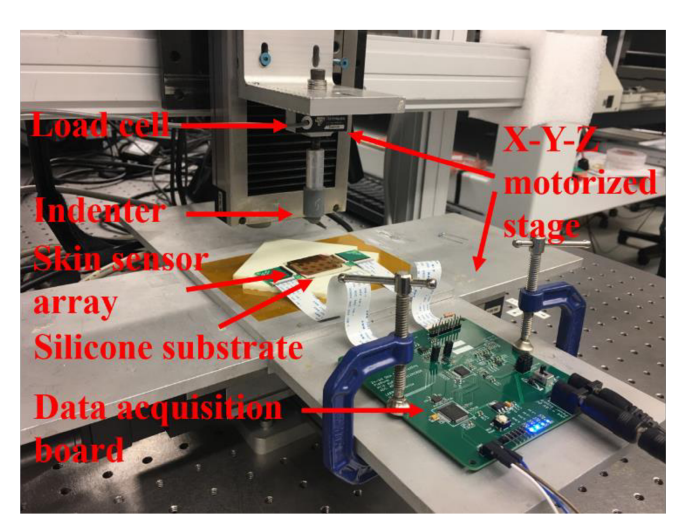


FIGURE 5: LAMINATION PROCESS FOR DOUBLE-LAYER SKIN SENSOR ARRAY

#### 3. HARDWARE SETUP FOR SENSOR TESTING

To measure the performance of the skin sensor array under various loading conditions, a custom-made indenter system was set up as shown in Figure 6. The testing system consists of three Newport® UTM150CC1HL motorized linear stages, which are assembled into an X-Y-Z platform. A load cell with a changeable indenter was mounted on the Z-axis to provide the load on the skin sensors, and a conditioning circuit was designed for receiving real-time strain data during load application. A MATLAB® graphical user interface was developed to collect data and visualize the strain gauge tactile response maps.



**FIGURE 6: SKIN SENSOR LOAD TESTING SYSTEM** 

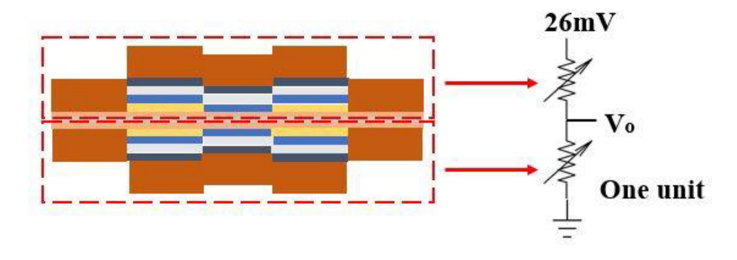
In the skin sensor patch, each sensing unit consists of two individual sensors that are physically stacked on each other, and electronically connected in series. Then, this unit is powered through a low-noise standard reference voltage source. The middle point of the two sensors is tapped by a 24-bit high resolution ADC module (Texas Instruments™, ADS1258) (shown in Figure 7) to detect any voltage fluctuation, which reflects the strain the unit experiences. The converted voltage signal is collected by a Microchip® microcontroller unit (MCU, model dsPIC33EP512MC806) and transferred to a PC through a UART to USB dongle.

The sensor patch is "trampolined" between the two Molex<sup>TM</sup> connectors (model 503480-3200). Within each sensing unit, the two sensor cells stack together "back-to-back". This configuration implies that when strain presents on one sensing unit, the two sensor cells deform or strain in opposite directions, hence resistance changes in "differential-mode" rather than "common-mode" (one increases and the other decreases). This effect essentially enhances the sensitivity of each sensing unit.

A buffered 26mV reference voltage is applied to the two resistors in series (the sensing unit). Ideally, the mid-point of the two resistors should output 13mV if the two sensor cells are identical. A 24-bit high resolution analog-to-digital converter (ADC) of ADS1258 from Texas Instrument<sup>TM</sup> was used to detect the mid-point voltage change, which all 16 input channels are multiplexed so that the input signals can be routed out of the IC, externally conditioned, and routed back to digitalize.

In our case, the ADC was operated under single-ended input, and bipolar power mode. Each input channel (AINx) of the ADC taps into a mid-point of the sensing unit, and a buffered 13mV DC signal is fed into the input common terminal (AINCOM) of the ADC. The 13mV is the expected resting voltage of the sensing unit, in an ideal world. We refer to this voltage as

baseline. Before a conversion happens, the internal multiplexer (MUX) routes the input voltage present at the AINx pin along with the 13mV baseline voltage present at the AINCOM pin out of the IC by MUXOUTP and MUXOUTN pins to an external instrumentation amplifier INA333, also from TI<sup>TM</sup>, to amplify the voltage difference



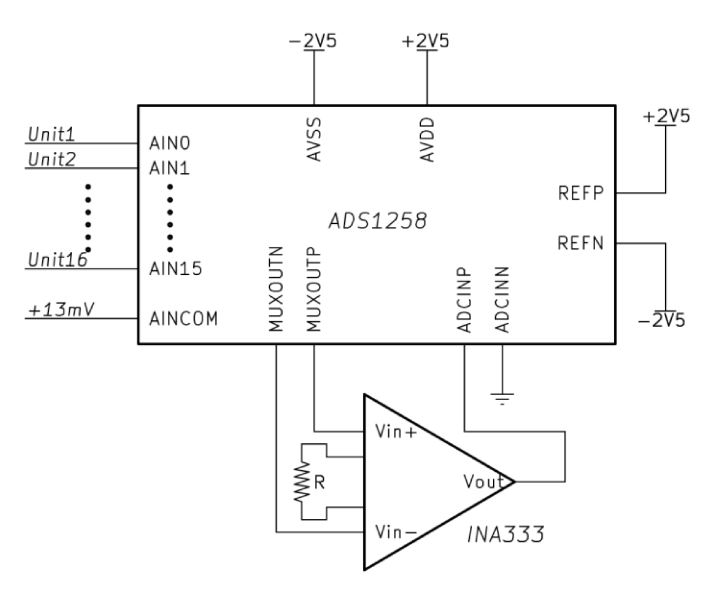


**FIGURE 7:** TOP: A PAIR OF SENSORS REPRESENT TWO POTENTIOMETERS IN SERIAL CONNECTION; BOTTOM: STRAIN SENSING CIRCUIT DIAGRAM. REFP, REFN PINS ARE THE REFERENCE VOLATAGE, AVDD IS THE POSITIVE SUPPLY AND THE AVSS IS THE NEGATIVE SUPPLY

#### 4. RESULTS AND DISCUSSION

Before doing the lamination of the sensor arrays, each single sensor's resistance is measured and recorded. This step is to prepare for two sensor arrays selection to laminate a double-side (back-to-back) sensor array. The selection is based on the corresponding resistance of sensors which are closed. As a double-side sensor array, two single sensors which are back to back laminated together become a pair. For this situation, those pairs are 2-10, 1-9, ..., 7-15, and 8-16 after back to back lamination. Figure 8 shows the arrangement of the sensors and electrodes of the sensor array, and the resistance of each sensor is listed in Table 1. Two single sensors' resistance of each pair are close, which is significant for temperature compensation.

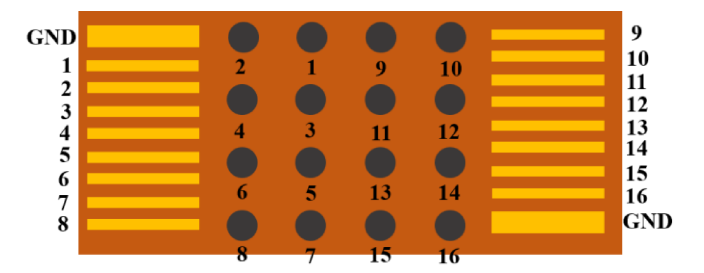


FIGURE 8: SENSORS AND ELECTRODES ARRANGEMENT OF A SENSOR ARRAY

**TABLE 1:** RESISTANCE MEASUREMENT OF TWO SENSOR ARRAYS OF A PAIR BEFORE LAMINATION

ARRAYS OF A PAIR BEFORE LAMINATION			
Number of	Resistance	Number of	Resistance
sensor	$(\Omega)$	sensor	$(\Omega)$
1	40.8	9	62.3
2	56.5	10	43.6
3	39.3	11	43.2
4	35.7	12	60.3
5	43.6	13	60.1
6	37.4	14	60.5
7	34.1	15	41.1
8	34.2	16	35.1
Number of	Resistance	Number of	Resistance
sensor	$(\Omega)$	sensor	$(\Omega)$
1	54.4	9	47.1
2	50.8	10	51.4
3	42.3	11	34.9
4	46.8	12	43.7
5	70.8	13	41.9
6	53.3	14	47.4
7	78.9	15	44.6
8	54.6	16	53.5

The sensor pair was placed on a soft Silicone substrate that deforms when subjected to pressure. When a load is applied on the sensor pair, the pair is squeezed by the pressure, the up-side sensor is compressed inwards, but bottom-side sensor is extended outwards. Strain is developed due to the bottom Silicone layer compliance, in addition to the double side laminate of the sensor.

Because of the piezoresistive material PEDOT:PSS between the star-shaped structures of sensor, the resistance of the two sensors of the pair are corresponding increasing (up-side) and decreasing (bottom-side) during the load applying. The ratio of resistance of the sensor pair is changed to make V<sub>0</sub> variable, so that the ADC signals from data acquisition board are varied and visualized the performances of the sensor strain gauge. With the variable load (0N-17.5N-0N) applied on the No. 5 sensor pair, the strain gauge performance of the No. 5 sensor pair and surrounding sensor pairs are shown in Figure 9. When the load reaches around 10N, other sensor pairs start to react with the load

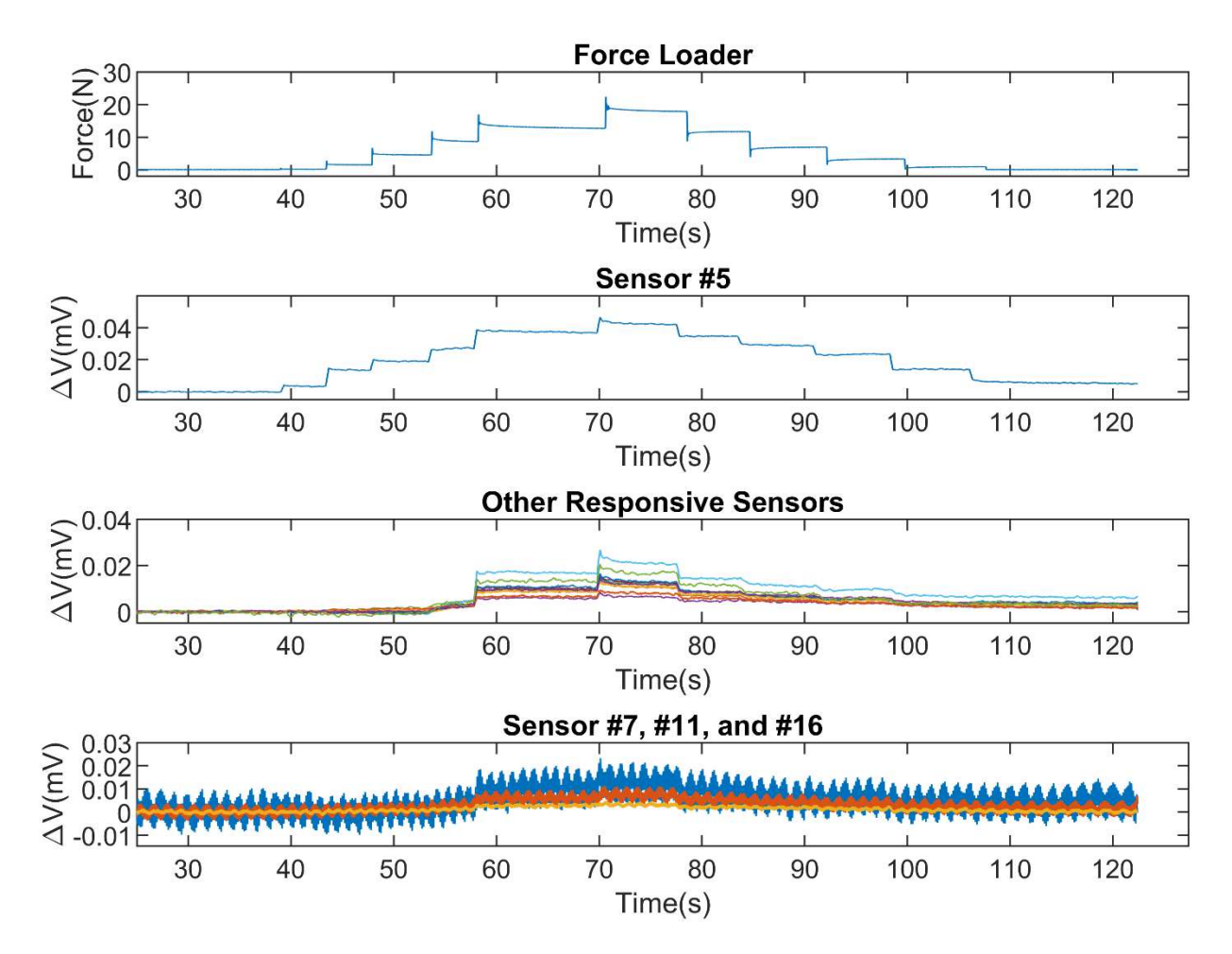


FIGURE 9: STRAIN GAUGE PERFORMANCE OF SENSOR PAIRS WITH VARIABLE LOAD APPLIED ON NO. 5 SENSOR

variation. Meanwhile, three sensor pairs, 7, 11, and 16 are less sensitive to the pressure of the load. This reduction of sensitivity may be due to the fact that lamination is still a manual process, thus prone to errors from the brayer and adhesive applicator.

#### 5. CONCLUSION

In this paper, we present a new fabrication process to create PEDOT:PSS organic piezoresistive robotic skins. Improvements to the sensor material formulation with DMSO and PVP were introduced, while a protective layer of Parylene and Titanium was proposed. The protective layer is used during dry etching to protect the tactile areas. Furthermore, a lamination process was introduced to create double-sided sensors for temperature compensation and increased load sensitivity. Using an electronic data acquisition board, we collected amplified signals from sensor pairs, and we used a MATLAB® interface to visualize the response of each sensor pair strain gauge during load application. The experimental results indicate 100% process yield after fabrication (16 tactile sensors out of 16), 82% yield after lamination (13 tactile sensors out of 16), results which are an improvement over prior work.

In the future, the lamination process should be improved to reduce operator errors. We will also investigate other additive manufacturing techniques to deposit PEDOT:PSS, such as Aerosol jetting.

#### **ACKNOWLEDGEMENTS**

This work was supported by National Science Foundation awards MRI #1828355 and EPSCOR #1849213. We would like to thank Joshua Baptist and the staffs of University of Louisville's Micro Nano Technology Center (MNTC) for their great suggestions and help in fabricating sensor samples.

#### **REFERENCES**

- [1] Bartolozzi, C., Natale, L., Nori, F., and Metta, G., 2016, "Robots with a sense of touch," Nature materials, 15(9), p. 921
- [2] Johnsson, M., and Balkenius, C., 2011, "Sense of touch in robots with self-organizing maps," IEEE Transactions on Robotics, 27(3), pp. 498-507.
- [3] Ward-Cherrier, B., Cramphorn, L., and Lepora, N. F., 2016, "Tactile manipulation with a TacThumb integrated on

- the open-hand M2 gripper," IEEE Robotics and Automation Letters, 1(1), pp. 169-175.
- [4] Mukai, T., Onishi, M., Odashima, T., Hirano, S., and Luo, Z., 2008, "Development of the tactile sensor system of a human-interactive robot "RI-MAN"," IEEE Transactions on robotics, 24(2), pp. 505-512.
- [5] Hoshi, T., and Shinoda, H., "Robot skin based on toucharea-sensitive tactile element," Proc. Proceedings 2006 IEEE International Conference on Robotics and Automation, 2006. ICRA 2006., IEEE, pp. 3463-3468.
- [6] Inaba, M., Hoshino, Y., Nagasaka, K., Ninomiya, T., Kagami, S., and Inoue, H., "A full-body tactile sensor suit using electrically conductive fabric and strings," Proc. Proceedings of IEEE/RSJ International Conference on Intelligent Robots and Systems. IROS'96, IEEE, pp. 450-457.
- [7] Lumelsky, V. J., Shur, M. S., and Wagner, S., 2001, "Sensitive skin," IEEE Sensors Journal, 1(1), pp. 41-51.
- [8] Wang, C., Hwang, D., Yu, Z., Takei, K., Park, J., Chen, T., Ma, B., and Javey, A., 2013, "User-interactive electronic skin for instantaneous pressure visualization," Nature materials, 12(10), p. 899.
- [9] Argall, B. D., and Billard, A. G., 2010, "A survey of tactile human-robot interactions," Robotics and autonomous systems, 58(10), pp. 1159-1176.
- [10] Dahiya, R. S., Metta, G., Valle, M., and Sandini, G., 2009, "Tactile sensing—from humans to humanoids," IEEE transactions on robotics, 26(1), pp. 1-20.
- [11] Saadatzi, M. N., Baptist, J. R., Yang, Z., and Popa, D. O., 2019, "Modeling and Fabrication of Scalable Tactile Sensor Arrays for Flexible Robot Skins," IEEE Sensors Journal.
- [12] Baptist, J., Zhang, R., Wei, D., Saadatzi, M., and Popa, D., "Fabrication of strain gauge sensor arrays for tactile skins," Proc. Proc. SPIE.
- [13] Das, S. K., Baptist, J. R., Sahasrabuddhe, R., Lee, W. H., and Popa, D. O., "Package analysis of 3D-printed piezoresistive strain gauge sensors," Proc. Sensors for Next-Generation Robotics III, International Society for Optics and Photonics, p. 985905.
- [14] Saadatzi, M. N., Baptist, J. R., Wijayasinghe, I. B., and Popa, D. O., "Characterization of large-area pressure sensitive robot skin," Proc. Smart Biomedical and Physiological Sensor Technology XIV, International Society for Optics and Photonics, p. 102160G.
- [15] Nothnagle, C., Baptist, J. R., Sanford, J., Lee, W. H., Popa, D. O., and Wijesundara, M. B., "EHD printing of PEDOT: PSS inks for fabricating pressure and strain sensor arrays on flexible substrates," Proc. Next-Generation Robotics II; and Machine Intelligence and Bio-inspired Computation: Theory and Applications IX, International Society for Optics and Photonics, p. 949403.
- [16] Saadatzi, M. N., Yang, Z., Baptist, J. R., Sahasrabuddhe, R. R., Wijayasinghe, I. B., and Popa, D. O., "Parametric investigation of scalable tactile sensors," Proc. Smart Biomedical and Physiological Sensor Technology

XIV, International Society for Optics and Photonics, p. 102160A.